Hindawi
International Journal of Antennas and Propagation
Volume 2019, Article ID 1657587, 12 pages
https://doi.org/10.1155/2019/1657587

Research Article

Evaluation of the Trapped Surface Wave of a Vertical Electric Dipole Based on Undetermined Coefficient Method in the Presence of *N*-Layered Region: A Graphical Approach

Hong Lei Xu,[1] Ting Ting Gu,[2] Yong Zhu,[1] Xiao Wei,[1] Liang Sheng Li,[1] and Hong Cheng Yin[1]

[1]*Science and Technology on Electromagnetic Scattering Laboratory, Beijing 100854, China*
[2]*Department of Information Science and Electronic Engineering, Zhejiang University, Hangzhou 310027, China*

Correspondence should be addressed to Hong Cheng Yin; yinhc207@126.com

Received 7 June 2019; Revised 21 August 2019; Accepted 20 September 2019; Published 20 October 2019

Academic Editor: Giuseppina Monti

In previous studies, the trapped surface wave, which is defined by the residue sums, has been addressed in the evaluation of the Sommerfeld integrals describing electromagnetic field of a vertical dipole in the presence of three-layered or four-layered region. But unfortunately, the existing computational scheme cannot provide analytical solution of the field in the presence of the *N*-layered region when $N > 4$. The scope of this paper is to overcome the limitations in root finding algorithm implied by the previous approach and provide solution of poles in stratified media. A set of pole equations following with explicit expressions are derived based on the undetermined coefficient method, which enable a graphical approach to obtain initial values of real roots. Accordingly, the generated trapped surface wave components are computed when both the observation point and the electric dipole source are on or near the surface of a dielectric-coated conductor. Validity, efficiency, and accuracy of the proposed method are illustrated by numerical examples.

1. Introduction

It is known that the electromagnetic fields radiated by a vertical or horizontal electric dipole in stratified media are interesting and practically important in many cases [1–3]. In the past decades, this problem has led to many published papers and available achievements on analytical solutions [4–21], especially the three-layered or four-layered cases.

The general integral representation of the electromagnetic field due to a dipole source has been addressed by King et al. [6] in the presence of the *N*-layered region, which was developed from the original expressions firstly formulated by Sommerfeld in 1909 [7] in the presence of half-spaces. Efforts have been made in a series of works [6–8] by investigators to derive analytical expressions for the Sommerfeld integrals, which leads to a better understanding of describing electromagnetic radiation from the dipole source than numerical solution, as well as time savings with respect to conventional techniques used to evaluate the integrals. In Chapter 15 of the monograph [6], the propagation of the electromagnetic pulses radiated by a horizontal electric dipole with delta-function excitation in the presence of the three-layered region was processed analytically, which demonstrated that the total field on or near the air-dielectric boundary is determined primarily by lateral wave, where the amplitude of the field along the boundary is $1/\rho^2$. Unfortunately, the integrals cannot be evaluated by means of the mentioned analytical procedure for electromagnetic field in the presence of the *N*-layered region.

In the comments by Wait and Mahoud et al. in 1998 [9, 10], and studies by other pioneers, particularly including Collin [11, 12] and Zhang and Pan [13], the three-layered structure was reconsidered by the use of asymptotic methods, contour integration, and branch cuts, where it is pointed out that the trapped surface wave, which is determined by residue sums of the poles, can be excited

efficiently by a dipole source with the amplitude of the field $1/\rho^{1/2}$ and should not be neglected over a dielectric-coated conductor [13]. To extend the study, the Sommerfeld integrals have been evaluated in the four-layered case by a similar method [14, 15], correspondingly. The details are summarized in a recent book by Li [16].

These new developments on the analytical results for the electromagnetic field in three-layered and four-layered structures [9–16], where it was proved that the trapped surface wave defined by the residue sums as the dominant wave propagates along the surface of air-dielectric boundary at long propagation distance [13], aroused interest in the study on properties of the trapped surface wave in the N-layered structure. However, few literatures relate to a computational scheme to solve the poles, for which the surface impedance at the air-dielectric boundary is in expression of a recursive form due to multireflections [6, 17]. Specially, the discrete pole root λ_j^* is hard to solve by analytical and numerical solutions due to multivalue properties of the recursive equation over four-layered media.

In a recent study by Cross, the solution of poles relying on numerical root finding algorithms is addressed in the four-layered structure to approximate the scenario of a leaking water-pipe, buried in the shallow subsurface [18], where it is suggested that the analytical solution of poles requires efficiency and enhancement of accuracies in stratified media.

Following the research line, we are attempting to derive the pole equation to release the difficulties in root finding in the N-layered structure. In the analysis, a set of pole equations with explicit expressions is developed for a computational scheme, so as to make it possible analytical evaluation of the trapped surface wave based on the undetermined coefficient method. The solution of obtained equations in three-layered to six-layered structures is carried out, respectively, as illustrative examples in lossless case by a graphical approach. The obtained equations offer advantages in terms of time savings with respect to standard pole equation in root finding procedures. In addition, computation and discussion are carried out by investigating the full-wave analytical expressions, as well as their interfering behaviour, which guarantees correctness by evaluating the residue sums' contributions to the fields, but also allows us to gain useful insight into the physics of the problem.

2. Formulation of the Problem

The 3D geometry under consideration and its 2D cylindrical coordinate system are shown in Figures 1 and 2, respectively, where the vertical electric dipole in the $\phi = 0$ direction is located at $(0, 0, d)$. Region $z > 0$ is the upper half-space occupied by air, and the lower half-space is composed of a success of $n + 1$ horizontal layers, each with arbitrary thickness $l_j\,(j = 1, 2, \ldots, n)$ and arbitrary wave number k_j, in which

$$k_0 = \omega\sqrt{\mu_0\varepsilon_0},$$
$$k_j = \omega\sqrt{\mu_0\left(\varepsilon_0\varepsilon_{rj} + \frac{i\sigma_j}{\omega}\right)}, \quad j = 1, 2, \ldots, n+1. \tag{1}$$

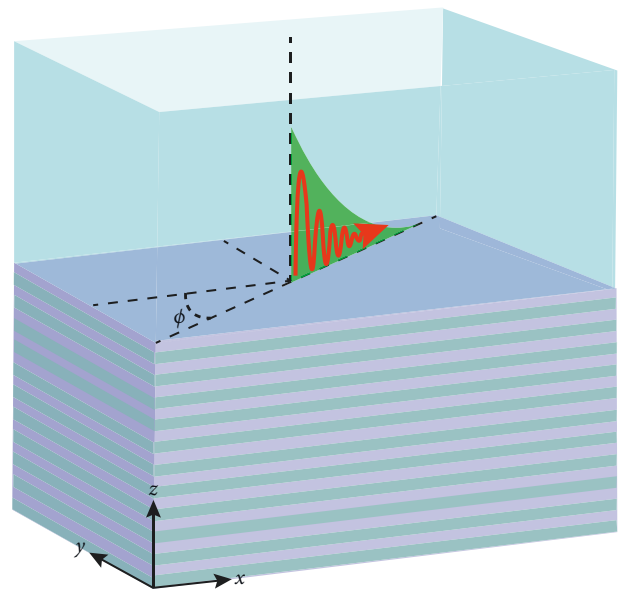

Figure 1: A multilayered model representing the simplest approximation of wave propagation.

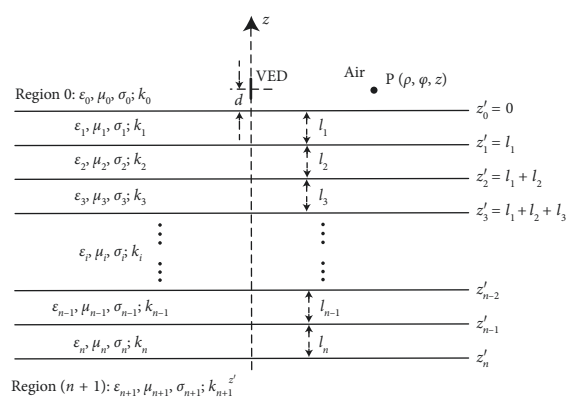

Figure 2: Geometrical profile of the horizontal N-layered model.

In the monograph by King et al. [6], the general integral formulas are addressed for the electromagnetic field due to a vertical electric dipole in the presence of N-layered media. The integrated formulas in Region 0 (Air) are written in forms of

$$B_{0\phi} = \frac{i\mu_0}{4\pi}\int_0^\infty \Big[e^{i\gamma_0|z-d|} + e^{i\gamma_0(z+d)} - (Q_n + 1)\,e^{i\gamma_0(z+d)}\Big]\gamma_0^{-1}J_1(\lambda\rho)\lambda^2\,\mathrm{d}\lambda, \tag{2}$$

$$E_{0\rho} = \frac{i\omega\mu_0}{4\pi k_0^2}\int_0^\infty \Big[\pm e^{i\gamma_0|z-d|} + e^{i\gamma_0(z+d)} - (Q_n + 1)e^{i\gamma_0(z+d)}\Big]J_1(\lambda\rho)\lambda^2\,\mathrm{d}\lambda, \quad \begin{cases} z \geq d, \\ 0 < z < d, \end{cases} \tag{3}$$

$$E_{0z} = -\frac{\omega\mu_0}{4\pi k_0^2}\int_0^\infty \left[e^{i\gamma_0|z-d|} + e^{i\gamma_0(z+d)} - (Q_n+1)e^{i\gamma_0(z+d)}\right]\gamma_0^{-1}J_0(\lambda\rho)\lambda^3 \mathrm{d}\lambda. \tag{4}$$

In aforementioned formulas, n represents for the number of intermediate dielectric layers and the reflection coefficient Q_n is expressed by

$$Q_n = -\frac{\gamma_0 - \left(k_0^2/(\omega\mu_0)\right)Z_{s0}(0)}{\gamma_0 + \left(k_0^2/(\omega\mu_0)\right)Z_{s0}(0)}, \tag{5}$$

in which $Z_{s0}(0)$ represents the surface impedance. If the procedure is continued to the boundary at $z' = z = 0$ between Region 0 and Region 1, the desired surface impedance is obtained. It is

$$\begin{aligned} Z'_{s0}(0) = \frac{\omega\mu_0\gamma_0}{k_0^2}\tanh\Bigg\{&\tanh^{-1}\left[\left(\frac{\gamma_1 k_0^2}{\gamma_0 k_1^2}\right)\tanh\left[-i\gamma_1 l_1\right.\right. \\ &+\tanh^{-1}\left[\left(\frac{\gamma_2 k_1^2}{\gamma_1 k_2^2}\right)\tanh\left[-i\gamma_2 l_2\right.\right. \\ &+\tanh^{-1}\left[\left(\frac{\gamma_3 k_2^2}{\gamma_2 k_3^2}\right)\tanh\left[-i\gamma_3 l_3 + \cdots\right.\right. \\ &+\tanh^{-1}\left[\left(\frac{\gamma_n k_{n-1}^2}{\gamma_{n-1} k_n^2}\right)\tanh\left[-i\gamma_n l_n\right.\right. \\ &\left.\left.\left.\left.\left.\left.+\tanh^{-1}\left(\frac{\gamma_{n+1}k_n^2}{\gamma_n k_{n+1}^2}\right)\right]\right]\cdots\right]\right]\right]\right]\Bigg\}, \end{aligned} \tag{6}$$

$$\gamma_i = \sqrt{k_i^2 - \lambda^2}; \quad i = 0, 1, 2, \ldots, n+1. \tag{7}$$

The first and second terms in (2)–(4) stand for the direct wave and the ideal reflected wave, respectively, and have been previously solved in [6] by King et al. Considering that γ_0 and γ_1 are functions of λ, which is made of the relations between Bessel and Hankel function:

$$\begin{aligned} J_n(\lambda\rho) &= \frac{1}{2}\left[H_n^{(1)}(\lambda\rho) + H_n^{(2)}(\lambda\rho)\right], \\ H_n^{(1)}(-\lambda\rho) &= H_n^{(2)}(\lambda\rho)(-1)^{n+1}. \end{aligned} \tag{8}$$

Thus, the third terms in (2)–(4) are rewritten as follows:

$$B_{0\phi}^{(3)} = -\frac{ik_0^2}{4\pi\omega}\int_{-\infty}^{\infty}\frac{Z_{s0}(0)H_1^{(1)}(\lambda\rho)e^{i\gamma_0(z+d)}\lambda^2}{\left[\gamma_0 + \left(k_0^2/(\omega\mu_0)\right)Z'_{s0}(0)\right]\gamma_0}\mathrm{d}\lambda, \tag{9}$$

$$E_{0\rho}^{(3)} = -\frac{i}{4\pi}\int_{-\infty}^{\infty}\frac{Z_{s0}(0)H_1^{(1)}(\lambda\rho)e^{i\gamma_0(z+d)\lambda^2}}{\gamma_0 + \left(k_0^2/(\omega\mu_0)\right)Z'_{s0}(0)}\mathrm{d}\lambda, \tag{10}$$

$$E_{0z}^{(3)} = \frac{1}{4\pi}\int_{-\infty}^{\infty}\frac{Z_{s0}(0)H_0^{(1)}(\lambda\rho)e^{i\gamma_0(z+d)}\lambda^3}{\left[\gamma_0 + \left(k_0^2/(\omega\mu_0)\right)Z'_{s0}(0)\right]\gamma_0}\mathrm{d}\lambda. \tag{11}$$

By similar treatment of asymptotic methods, contour integration and branch cuts applied in three-layered and four-layered structures, which is addressed in detail by Li [16], the terms from (9)–(11) can be considered as the combination of the branch cut integrals and contribution of the residues of poles, which are defined by the trapped-surface-wave-term and the lateral-wave-term, respectively. It is necessary to shift the contours around all the branches at $\lambda_1 = k_0$, $\lambda_2 = k_1$, …, $\lambda_j = k_{n+1}$, respectively. Since the approximation of each branch cut integral refers to a lot of mathematical derivations, which is beyond the main scope of this paper, the lateral-wave-term is not addressed in illustrative examples for simplicity. In the next, attention is made on evaluation of the trapped-surface-wave-term by inviting analytical techniques to evaluate the discrete pole residues.

3. Evaluation of the Trapped Surface Wave in the Presence of the *N*-Layered Region

3.1. Residue of the Poles for the Trapped-Surface-Wave-Term. Following the integration procedure addressed in [16], the trapped-surface-wave-term is defined by the sum of pole residues. In the N-layered structure, the terms of trapped surface wave due to a vertical electric dipole are written as

$$\begin{aligned} B_{0\phi}^{\mathrm{Sur}} &= \frac{k_0^2}{2\omega}\sum_j \frac{Z'_{s0}(\lambda_j^*)H_1^{(1)}(\lambda_j^*\rho)e^{i\gamma_0(\lambda_j^*)(z+d)}(\lambda_j^*)^2}{q'_N(\lambda_j^*)\gamma_0(\lambda_j^*)}, \\ E_{0\rho}^{\mathrm{Sur}} &= \frac{1}{2}\sum_j \frac{Z'_{s0}(\lambda_j^*)H_1^{(1)}(\lambda_j^*\rho)e^{i\gamma_0(\lambda_j^*)(z+d)}(\lambda_j^*)^2}{q'_N(\lambda_j^*)}, \\ E_{0z}^{\mathrm{Sur}} &= \frac{i}{2}\sum_j \frac{Z'_{s0}(\lambda_j^*)H_0^{(1)}(\lambda_j^*\rho)e^{i\gamma_0(\lambda_j^*)(z+d)}(\lambda_j^*)^3}{q'_N(\lambda_j^*)\gamma_0(\lambda_j^*)}, \end{aligned} \tag{12}$$

in which the function q'_N is expressed by

$$q'_N = \frac{\partial}{\partial\lambda}\left[\gamma_0 + \left(\frac{k_0^2}{\omega\mu_0}\right)Z'_{s0}(0)\Big|_{n=N-2}\right], \tag{13}$$

and λ_j^* $(j = 1, 2, \ldots)$ are the discrete roots of the pole equation of the electromagnetic field in the presence of the N-layered region, which is in a variant of the surface impedance function $Z'_{s0}(0)$ at the air-to-dielectric boundary where $n = N-2$ represents the number of intermediate dielectric layers of the N-layered structure, written as

$$q_N = \gamma_0 + \left(\frac{k_0^2}{\omega\mu_0}\right)Z'_{s0}(0)\Big|_{n=N-2} = 0. \tag{14}$$

Considering the pole equation by (14) with substitution of (6) in the form of a recursive expression, it is necessary to derive the explicit pole equation first. Suppose (14) can be rewritten with respect to the function $G_N^{(n)}$, so that

$$q_N = \gamma_0 + \frac{\gamma_1 k_0^2}{k_1^2}G_N^{(n)}(\lambda) = 0, \tag{15}$$

in which $G_N^{(n)}$ is defined by

$$G_N^{(n)}(\lambda) = \frac{k_1^2}{\omega\mu_0\gamma_1} Z'_{s0}(0). \tag{16}$$

The superscript n of function $G_N^{(n)}$ represents the recursive order of the function that is in a variant of λ. In the meanwhile, (15) can be expanded if the order $n \geq 1$ by taking into account of (6) with the function $G_N^{(n-1)}$. Specifically, it is expressed by a set of sequential equations, as follows:

$$\begin{aligned}
q|_{N=2} &= \gamma_0 + \frac{\gamma_1 k_0^2}{k_1^2} G_2^{(0)}(\lambda), \\
q|_{N=3} &= \gamma_0 + \frac{\gamma_1 k_0^2}{k_1^2} G_3^{(1)}(\lambda) \\
&= \gamma_0 + \frac{\gamma_1 k_0^2}{k_1^2} \tanh\left[-i\gamma_1 l_1 + \tanh^{-1}\left(\frac{\gamma_2 k_1^2}{\gamma_1 k_2^2}\right) G_3^{(0)}(\lambda)\right], \\
q|_{N=4} &= \gamma_0 + \frac{\gamma_1 k_0^2}{k_1^2} G_4^{(2)}(\lambda) \\
&= \gamma_0 + \frac{\gamma_1 k_0^2}{k_1^2} \tanh\left[-i\gamma_1 l_1 + \tanh^{-1}\left(\frac{\gamma_2 k_1^2}{\gamma_1 k_2^2}\right) G_4^{(1)}(\lambda)\right] \\
&= \gamma_0 + \frac{\gamma_1 k_0^2}{k_1^2} \tanh\left[-i\gamma_1 l_1 + \tanh^{-1}\left[\left(\frac{\gamma_2 k_1^2}{\gamma_1 k_2^2}\right)\right.\right. \\
&\quad \left.\left. \cdot \tanh\left[-i\gamma_2 l_2 + \tanh^{-1}\left(\frac{\gamma_3 k_2^2}{\gamma_2 k_3^2}\right) G_4^{(0)}(\lambda)\right]\right]\right], \\
&\cdots \\
q|_N &= \gamma_0 + \frac{\gamma_1 k_0^2}{k_1^2} G_N^{(n)}(\lambda) \\
&= \gamma_0 + \frac{\gamma_1 k_0^2}{k_1^2} \tanh\left[-i\gamma_1 l_1 + \tanh^{-1}\left(\frac{\gamma_2 k_1^2}{\gamma_1 k_2^2}\right) G_N^{(n-1)}(\lambda)\right].
\end{aligned} \tag{17}$$

It is seen from equation (17) that the recursive order n of function $G_N^{(n)}$ is reduced if the following identity is satisfied:

$$G_N^{(j+1)}(\lambda) = \tanh\left[-i\gamma_m l_m + \tanh^{-1}\left(\frac{\gamma_{m+1} k_m^2}{\gamma_m k_{m+1}^2} G_N^{(j)}(\lambda)\right)\right], \quad m = N - j - 1. \tag{18}$$

Combining equations from (17), it is inferred that $G_N^{(j)}(\lambda)|_{j=0} \equiv 1$ is applied in each equation when $n = N - 2$. Consequently, the equations are adapted by exploiting both (18) and $G_N^{(j)}(\lambda)|_{j=0} \equiv 1$, as follows:

$$\begin{aligned}
N = 3 &: \tanh(i\gamma_1 l_1) + G_3^{(0)}(\lambda) \\
&= \frac{\gamma_2 k_1^2}{\gamma_1 k_2^2} + G_3^{(0)}(\lambda) \frac{\gamma_2 k_1^2}{\gamma_1 k_2^2} \tanh(i\gamma_1 l_1), \quad \text{when } G_3^{(0)}(\lambda) = 1,
\end{aligned} \tag{19}$$

$$\begin{aligned}
N = 4 &: \tanh(i\gamma_2 l_2) + G_4^{(1)}(\lambda) \\
&= \frac{\gamma_2 k_1^2}{\gamma_1 k_2^2} + G_4^{(1)}(\lambda) \frac{\gamma_2 k_1^2}{\gamma_1 k_2^2} \tanh(i\gamma_2 l_2), \quad \text{when } G_4^{(0)}(\lambda) = 1,
\end{aligned} \tag{20}$$

$$\begin{aligned}
N = 5 &: \tanh(i\gamma_3 l_3) + G_5^{(2)}(\lambda) \\
&= \frac{\gamma_2 k_1^2}{\gamma_1 k_2^2} + G_5^{(2)}(\lambda) \frac{\gamma_2 k_1^2}{\gamma_1 k_2^2} \tanh(i\gamma_3 l_3), \quad \text{when } G_5^{(0)}(\lambda) = 1, \\
&\cdots
\end{aligned} \tag{21}$$

In (19), the explicit expression of pole equation in the three-layered structure is easy to obtain by $G_3^{(0)} = 1$. Similarly, for general case with $n > 3$, such as in the four-layered and five-layered structures by (20) and (21), respectively, where the function $G_N^{(n-1)}$ with respect to the variable λ has been applied, the explicit equation is defined by suppressing $G_N^{(0)} = 1$. Through mathematical derivations, the variant coefficients are derived accordingly in expression of recursive form, as follows:

$$\begin{aligned}
N \geq 4 &: G_3^{(0)}(\lambda) = -\frac{\gamma_0 k_1^2}{\gamma_1 k_0^2}, \\
N \geq 5 &: G_4^{(1)}(\lambda) = \frac{\tanh(i\gamma_1 l_1) + G_3^{(0)}(\lambda)}{(\gamma_2 k_1^2/\gamma_1 k_2^2) + G_3^{(0)}(\lambda)(\gamma_2 k_1^2/\gamma_1 k_2^2)\tanh(i\gamma_1 l_1)}, \\
N \geq 6 &: G_5^{(2)}(\lambda) = \frac{\tanh(i\gamma_2 l_2) + G_4^{(1)}(\lambda)}{(\gamma_3 k_2^2/\gamma_2 k_3^2) + G_4^{(1)}(\lambda)(\gamma_3 k_2^2/\gamma_2 k_3^2)\tanh(i\gamma_2 l_2)}. \\
&\cdots
\end{aligned} \tag{22}$$

Therefore, it is concluded that the general expression of pole equation for electromagnetic field in the presence of N-layered region is derived from (14), in expression of

$$\begin{aligned}
\tanh(i\gamma_n l_n) + G_N^{(n-1)}(\lambda) &= \frac{\gamma_2 k_1^2}{\gamma_1 k_2^2} \\
&+ G_N^{(n-1)}(\lambda) \frac{\gamma_2 k_1^2}{\gamma_1 k_2^2} \tanh(i\gamma_n l_n), \quad \text{when } G_N^{(0)} = 1,
\end{aligned} \tag{23}$$

where

$$G_N^{(j)}(\lambda) = \frac{\tanh\left(i\gamma_j l_j\right) + G_N^{(j-1)}(\lambda)}{\left(\gamma_{j+1}k_j^2/\gamma_j k_{j+1}^2\right) + G_N^{(j-1)}(\lambda)\left(\gamma_{j+1}k_j^2/\gamma_j k_{j+1}^2\right)\tanh\left(i\gamma_j l_j\right)}. \tag{24}$$

3.2. Solution of Poles: A Graphical Approach. In order to evaluate the pole residues analytically, the set of equations from (19)–(21) are developed into explicit expressions with substitution of equations from (22). For convenience, the pole equation in the presence of three-layered region obtained from (19) is rewritten as

$$N = 3: \ \tanh\left(i\gamma_1 l_1\right) = \frac{\gamma_2 k_1^2}{\gamma_1 k_2^2} + \frac{\gamma_0 k_1^2}{\gamma_1 k_0^2} - \frac{\gamma_0 k_1^2}{\gamma_1 k_0^2}\frac{\gamma_2 k_1^2}{\gamma_1 k_2^2}\tanh\left(i\gamma_1 l_1\right). \tag{25}$$

Analogously, the pole equation is derived for electromagnetic field of a vertical electric dipole in the presence of N-layered region by substituting (23) with (24), iteratively. Specifically, the pole equations for the fields in the four-layered to six-layered structures can be written as follows:

$$\begin{aligned} N = 4: \ \tanh\left(i\gamma_2 l_2\right) &= \frac{\gamma_3 k_2^2}{\gamma_2 k_3^2} + \left(\frac{\gamma_1 k_2^2}{\gamma_2 k_1^2}\cdot\frac{\gamma_1 k_0^2}{\gamma_0 k_1^2}\right) \\ &\times \frac{\tanh\left(i\gamma_1 l_1\right) - A_1(\lambda)}{\tanh\left(i\gamma_1 l_1\right) - B_1(\lambda)} - \frac{\gamma_3 k_2^2}{\gamma_2 k_3^2}\left(\frac{\gamma_1 k_2^2}{\gamma_2 k_1^2}\cdot\frac{\gamma_1 k_0^2}{\gamma_0 k_1^2}\right) \\ &\times \frac{\tanh\left(i\gamma_1 l_1\right) - A_1(\lambda)}{\tanh\left(i\gamma_1 l_1\right) - B_1(\lambda)}\cdot \tanh\left(i\gamma_2 l_2\right), \end{aligned} \tag{26}$$

$$\begin{aligned} N = 5: \ \tanh\left(i\gamma_3 l_3\right) &= \frac{\gamma_4 k_3^2}{\gamma_3 k_4^2} + \left(\frac{\gamma_2 k_3^2}{\gamma_3 k_2^2}\cdot\frac{\gamma_0 k_1^2}{\gamma_1 k_0^2}\right) \\ &\times \frac{\tanh\left(i\gamma_2 l_2\right) - A_2(\lambda)}{\tanh\left(i\gamma_2 l_2\right) - B_2(\lambda)} - \frac{\gamma_4 k_3^2}{\gamma_3 k_4^2}\left(\frac{\gamma_2 k_3^2}{\gamma_3 k_2^2}\cdot\frac{\gamma_0 k_1^2}{\gamma_1 k_0^2}\right) \\ &\times \frac{\tanh\left(i\gamma_2 l_2\right) - A_2(\lambda)}{\tanh\left(i\gamma_2 l_2\right) - B_2(\lambda)}\cdot \tanh\left(i\gamma_3 l_3\right), \end{aligned} \tag{27}$$

$$\begin{aligned} N = 6: \ \tanh\left(i\gamma_4 l_4\right) &= \frac{\gamma_5 k_4^2}{\gamma_4 k_5^2} + \left(\frac{\gamma_3 k_4^2}{\gamma_4 k_3^2}\cdot\frac{\gamma_0 k_1^2}{\gamma_1 k_0^2}\right) \\ &\times \frac{\tanh\left(i\gamma_3 l_3\right) - A_3(\lambda)}{\tanh\left(i\gamma_3 l_3\right) - B_3(\lambda)} - \frac{\gamma_5 k_4^2}{\gamma_4 k_5^2}\left(\frac{\gamma_3 k_4^2}{\gamma_4 k_3^2}\cdot\frac{\gamma_0 k_1^2}{\gamma_1 k_0^2}\right) \\ &\times \frac{\tanh\left(i\gamma_3 l_3\right) - A_3(\lambda)}{\tanh\left(i\gamma_3 l_3\right) - B_3(\lambda)}\cdot \tanh\left(i\gamma_4 l_4\right). \end{aligned} \tag{28}$$

...

By a few mathematical efforts, the functions $A_j(\lambda)$ and $B_j(\lambda)$ from (26)–(28) are derived through iterative substitutions, which are listed in Appendix, correspondingly. It is noted that the pole equation can be expressed in analogous form for the electromagnetic field of a vertical dipole in the presence of N-layered media. Accordingly, substituting the equations from (26)–(28) with functions $A_j(\lambda)$, the explicit expression of equations are obtained. By transpositions and rearrangements, the expression of pole equation in the presence of N-layered region can be described as

$$\begin{aligned} &\left[1 + \frac{\gamma_{n+1}k_n^2}{\gamma_n k_{n+1}^2}\cdot\frac{\gamma_{n-1}k_n^2}{\gamma_n k_{n-1}^2}\cdot\frac{\sum_{m=1}^{n-1}\prod_{j=1}^{m}C_n^*(j,m)\tanh\left(i\gamma_j l_j\right)}{\sum_{k=1}^{n-1}\prod_{j=1}^{m}C_n^*(m-j,n-m)\tanh\left(i\gamma_j l_j\right)}\right] \\ &\quad\cdot \tanh\left(i\gamma_n l_n\right) \\ &= \frac{\gamma_{n+1}k_n^2}{\gamma_n k_{n+1}^2} + \frac{\gamma_{n-1}k_n^2}{\gamma_n k_{n-1}^2} \\ &\quad\cdot \frac{1 - \sum_{m=1}^{n-1}\prod_{j=1}^{m}C_n^*(j,m)\tanh\left(i\gamma_j l_j\right)}{\sum_{m=1}^{n-1}\prod_{j=1}^{m}C_n^*(m-j,n-m)\tanh\left(i\gamma_j l_j\right)}, \end{aligned} \tag{29}$$

in which the coefficients $C_n^*(j,m)$, $j = 1, \ldots, m$; $m = 1, \ldots, n$ are a set of coefficients defined by positive or negative ratio of $\gamma_j k_m$ and $\gamma_m k_j$, which are determined from (26)–(28). If the bottom half-space is considered as perfectly conducting layer as depicted in Figure 3, the expression of (29) are simplified in condition of $k_{n+1} \longrightarrow \infty$, which reduces to

$$\tanh\left(i\gamma_n l_n\right) = \frac{\gamma_{n-1}k_n^2}{\gamma_n k_{n-1}^2}\cdot\frac{1 - \sum_{m=1}^{n-1}\prod_{j=1}^{m}C_n^*(j,m)\tanh\left(i\gamma_j l_j\right)}{1 - \sum_{m=1}^{n-1}\prod_{j=1}^{m}C_n^*(m-j,n-m)\tanh\left(i\gamma_j l_j\right)}. \tag{30}$$

It is seen from (29) and (30) that the obtained equations for the fields are expressed in form of addition, subtraction, and multiplication of functions $\tanh\left(i\gamma_j l_j\right)$ with coefficients C_n^*, which offer advantages in terms of time savings with respect to standard numerical root finding procedures by (14). Specifically, the obtained pole equations for the electromagnetic field over a conductor coated by two-layered to four-layered dielectrics are in terms of the following equations:

$$N = 4: \ \tanh\left(i\gamma_2 l_2\right) = \left(\frac{\gamma_1 k_2^2}{\gamma_2 k_1^2}\cdot\frac{\gamma_1 k_0^2}{\gamma_0 k_1^2}\right)\frac{\tanh\left(i\gamma_1 l_1\right) - A_1(\lambda)}{\tanh\left(i\gamma_1 l_1\right) - B_1(\lambda)}, \tag{31}$$

$$N = 5: \ \tanh\left(i\gamma_3 l_3\right) = \left(\frac{\gamma_2 k_3^2}{\gamma_3 k_2^2}\cdot\frac{\gamma_0 k_1^2}{\gamma_1 k_0^2}\right)\frac{\tanh\left(i\gamma_2 l_2\right) - A_2(\lambda)}{\tanh\left(i\gamma_2 l_2\right) - B_2(\lambda)}, \tag{32}$$

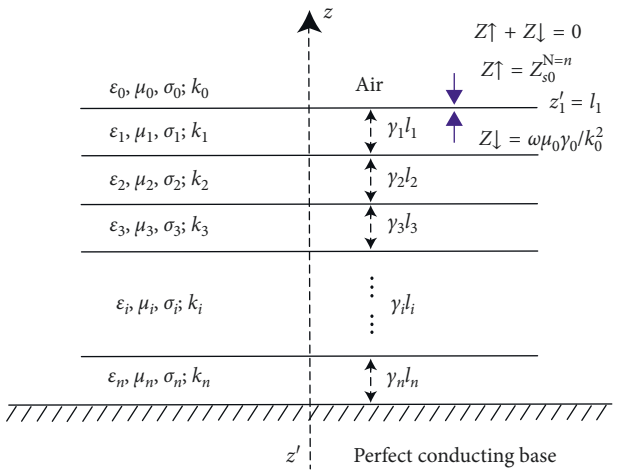

Figure 3: The N-layered model with the bottom half-space as conducting.

$$N = 6: \ \tanh(i\gamma_4 l_4) = \left(\frac{\gamma_3 k_4^2}{\gamma_4 k_3^2} \cdot \frac{\gamma_0 k_1^2}{\gamma_1 k_0^2}\right) \frac{\tanh(i\gamma_3 l_3) - A_3(\lambda)}{\tanh(i\gamma_3 l_3) - B_3(\lambda)}. \quad (33)$$

$$\ldots$$

It is convenient to validate (31) in derivation followed, which is exactly the same with (4.24) presented in [16] for the electromagnetic field of a vertical electric dipole on the surface of a conductor coated by two dielectric layers.

$$\begin{aligned} q_{N=4}^{\text{Per}} &= \gamma_0 - i\frac{\gamma_1 k_0^2}{k_1^2}\tan\left[\gamma_1 l_1 + \tanh^{-1}\left[\left(\frac{\gamma_2 k_1^2}{\gamma_1 k_2^2}\right)\tan(\gamma_2 l_2)\right]\right] \\ &= \gamma_0 - i\frac{\gamma_1 k_0^2}{k_1^2}\left[\tan(\gamma_1 l_1) + \left(\frac{\gamma_2 k_1^2}{\gamma_1 k_2^2}\right)\tan(\gamma_2 l_2)\right] \\ &\quad \times \left[1 - \frac{\gamma_2 k_1^2}{\gamma_1 k_2^2}\tan(\gamma_1 l_1)\tan(\gamma_2 l_2)\right]^{-1} = 0. \end{aligned} \quad (34)$$

Through the aforementioned analysis, the computational scheme to evaluate the residue sums for the trapped surface wave is proposed by exploiting the derived equations from (25)–(28). A graphical approach is applied in the present study to obtain initial values of real roots. For instance of a five-layered structure interpreted in Figure 4, the real roots are obtained from intersections of functions $f(\lambda)$ and $g(\lambda)$, where the intermediate dielectric layers are assumed to be lossless.

$$\begin{aligned} f_{N=5}(\lambda) &= \tan(\gamma_3 l_3); \\ g_{N=5}(\lambda) &= \frac{\text{right side of equation (27)}}{i}. \end{aligned} \quad (35)$$

4. Computation and Discussion

4.1. Illustrative Examples by a Graphical Approach. Primary objective of this section is to show the graphical approach to evaluate the poles by equations from (25)–(28) representing the three-layered to six-layered structures,

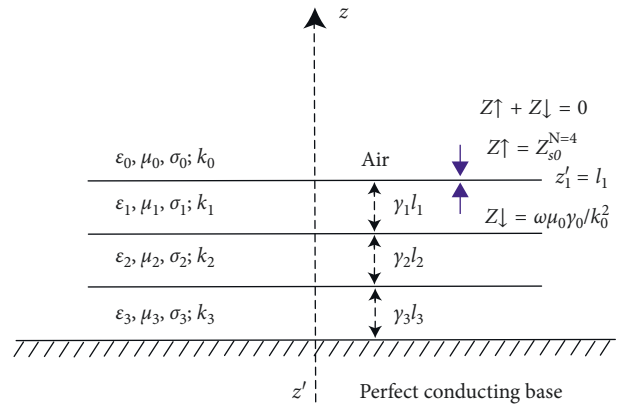

Figure 4: A five-layered model with the bottom half-space as perfectly conducting.

respectively. In Figure 5 and 6, the real roots are obtained in lossless case, where the bottom half-space is considered as perfectly conducting and the electric lengths of intermediate dielectrics are identical. The computation coefficients of relative permittivity in the intermediate dielectrics are chosen by $\varepsilon_{r1} = 2.65$, $\varepsilon_{r2} = 4.0$, $\varepsilon_{r3} = 6.0$, and $\varepsilon_{r4} = 8.0$, respectively, where each electric length of the intermediate dielectrics are chosen by $k_i l_i = 0.45\pi$ and $k_i l_i = 1.45\pi$, respectively.

As illustrated in Figure 5, the roots of equations from (25) to (27) are obtained from intersections of functions $\tan(\gamma_n l_n)$ and the right side terms $g_N(\lambda)$ on the condition of $k_{n+1} \longrightarrow \infty$. It is seen from Figures 5(c)–5(h), the terms of right side of (27)/i representing five-layered structure have imaginary part in the region of $k_1 \le \gamma_j^* \le k_2$, since the function $\gamma_1 = (k_1^2 - \gamma_j^{*2})^{1/2}$ is imaginary in the region of $\gamma_j > k_1$. In Figure 6, the roots of (28) are plotted on condition of $k_5 \longrightarrow \infty$ for electromagnetic field of a vertical dipole in the six-layered structure. In the computations, the intermediate dielectrics are chosen as lossless and the bottom half-space is perfectly conducting, whereas in the general cases where the roots may not be always real, the resulted roots are considered as initial values for numerical iterations.

In Figure 7, by applying the roots of poles, the electromagnetic field of a vertical dipole is computed, correspondingly. The total field, the trapped surface wave, and DRL waves (direct wave, reflected waves, and lateral wave) are computed with the same parameters in Figures 5(b) and 5(f), respectively, at the operating frequency $f = 100$ MHz. It is seen from Figure 7 that the trapped surface wave propagates along the air-to-dielectric boundary as the dominate wave on the condition of $k_1 < k_2 < k_3$, and $k_3 \longrightarrow \infty$, in the presence of four-layered region. When $k_0 < \lambda < k_1$, $\gamma_j(\lambda) = i(\lambda^2 - k_j^2)^{1/2}$ is always a positive imaginary number, and the terms including the factor will attenuate exponentially as in the z direction. In Figure 8, the curves of the trapped surface wave versus propagation distance are plotted in three-layered to five-layered structures, respectively, when both the observation point and dipole source are placed on the surface of air-dielectric boundary. The electric lengths of each layer of intermediate dielectrics are identical with

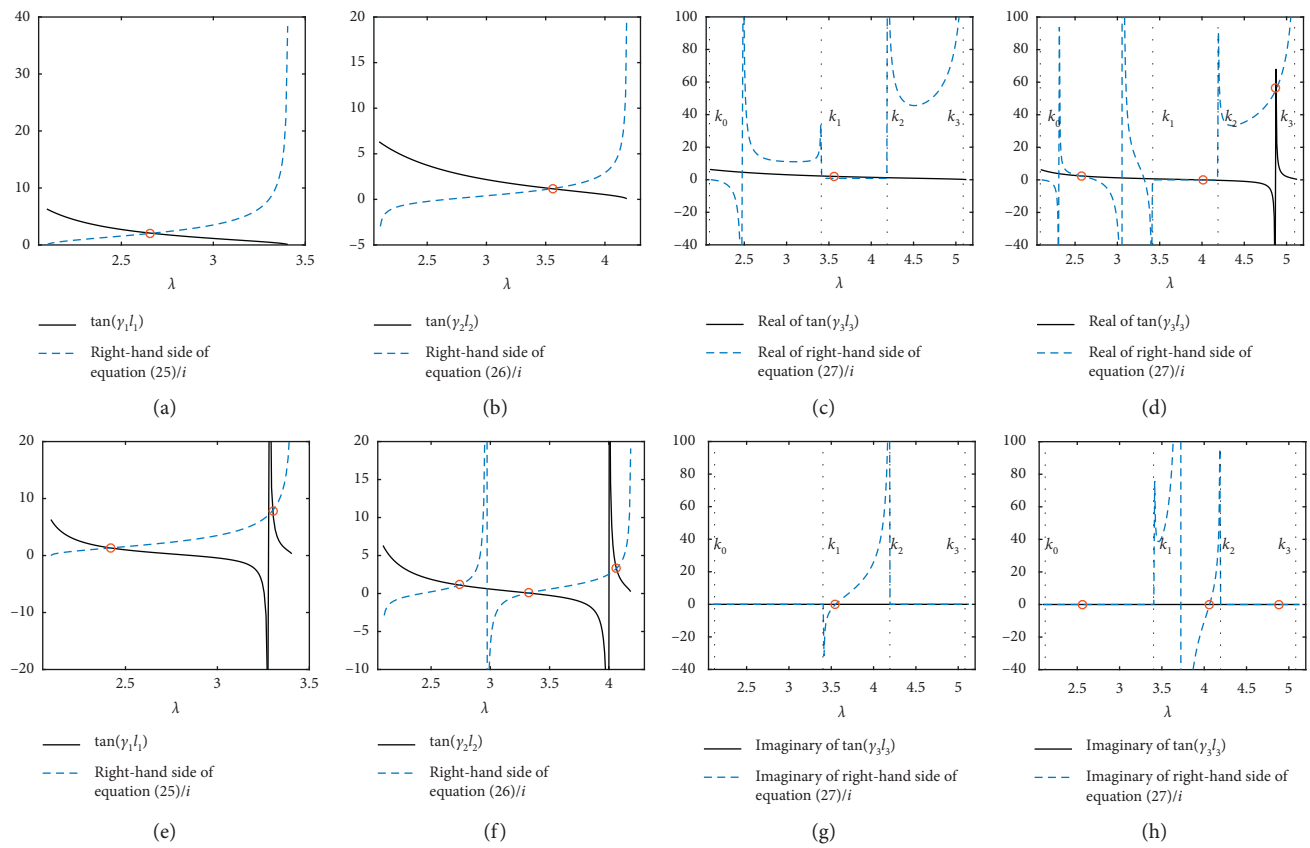

Figure 5: Graphical approach for root finding in evaluations of poles by equations from (25)–(27) at the operating frequency $f = 100$ MHz for the electromagnetic field due to a vertical dipole over a perfect conductor coated by multilayered lossless dielectrics, with (a) $N = 3$, $k_i l_i = 0.45\pi$; (b) $N = 4$, $k_i l_i = 1.45\pi$; (c) $N = 5$, $k_i l_i = 0.45\pi$; (d) $N = 5$, $k_i l_i = 1.45\pi$; (e) $N = 3$, $k_i l_i = 1.45\pi$; (f) $N = 4$, $k_i l_i = 1.45\pi$; (g) $N = 5$, $k_i l_i = 0.45\pi$; and (h) $N = 5$, $k_i l_i = 1.45\pi$.

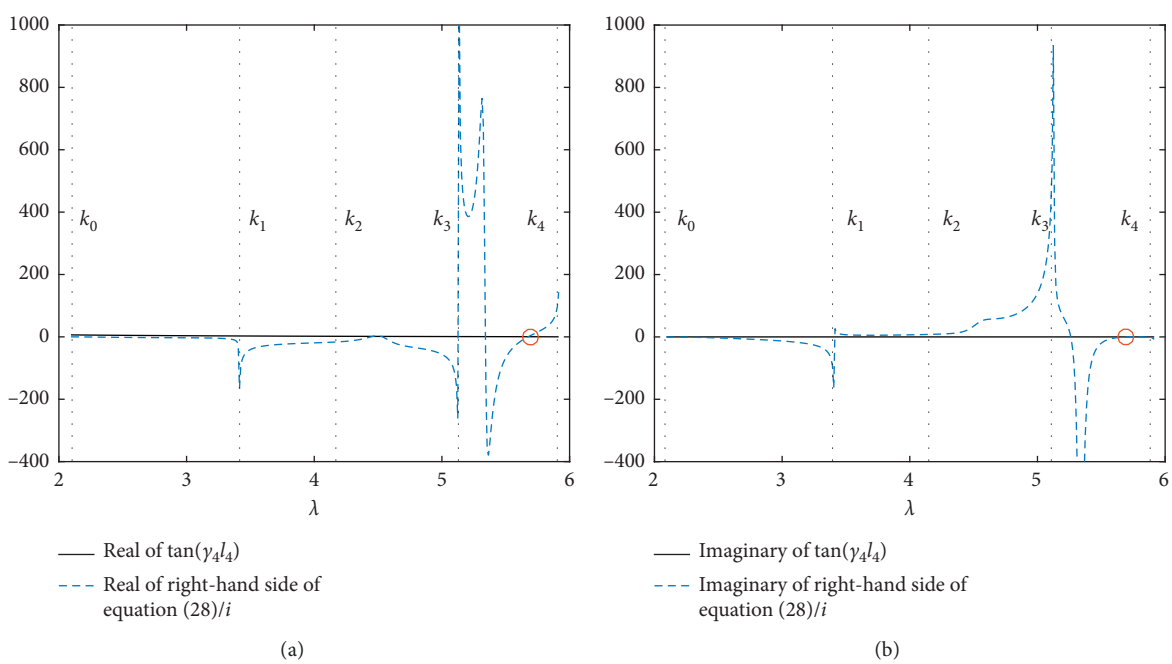

Figure 6: Continued.

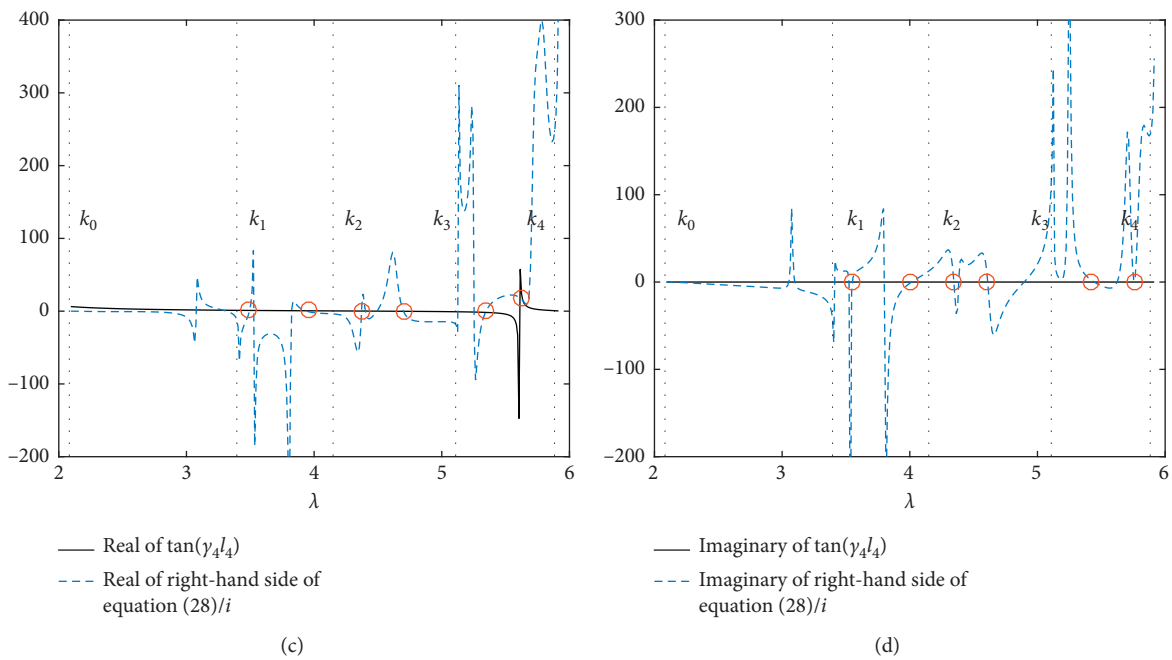

Figure 6: Graphical approach for root finding in evaluations of poles by (33) for the electromagnetic field due to a vertical dipole over a perfect conductor coated by four-layered lossless dielectrics, with (a) $k_i l_i = 0.45\pi$; (b) $k_i l_i = 0.45\pi$; (c) $k_i l_i = 1.45\pi$; and (d) $k_i l_i = 1.45\pi$.

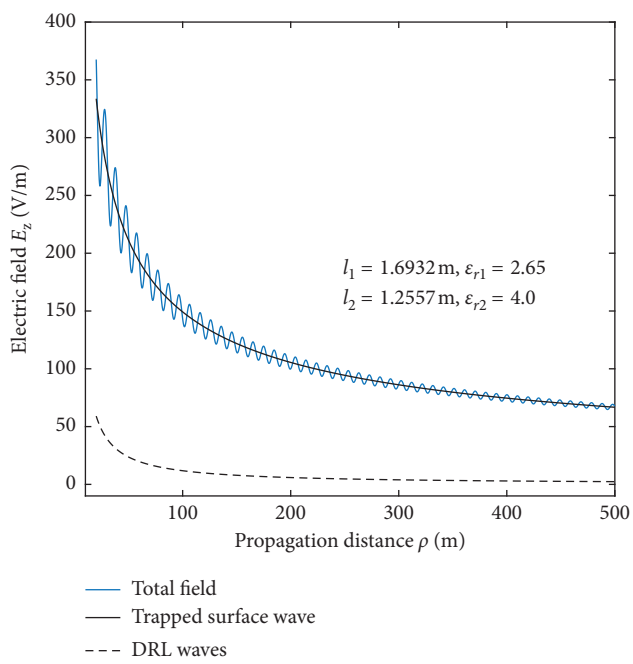

Figure 7: The electric component $|E_{0z}(\rho, z)|$ of electromagnetic field due to a vertical dipole on the conductor coated by two dielectric layers.

$k_i l_i = 0.45\pi$. It is seen that field strength for trapped surface wave disperses as increased by layers of coating dielectrics.

One would ask whether the derived equation in expression of (23) is advantageous in terms of computation over previous numerical procedures. This aspect is illustrated in Table 1, which shows the computation complexity and nested recursion times taken by the proposed method, and the previous numerical solution, to calculate the poles of the trapped surface wave generated by a vertical electric dipole lying on a horizontal layered medium at $z = 0$.

4.2. Interfering Behaviour of the Electromagnetic Field above the Surface of a Dielectric-Coated Conductor. To investigate the propagation properties of the electromagnetic field of a vertical electric dipole over a dielectric-coated conductor, the spatial distributions in $\hat{\rho} - \hat{z}$ plane are plotted in Figures 9 to 11 at the operating frequency $f = 100$ MHz, when both the observation point and radiating source are located at the surface of air-dielectric boundary. In Figure 9, the DR fields (including the direct wave and ideal reflected wave) are computed by the first two terms in equations from (2)–(4). It is noted that the DR terms in the multilayered structures are the same with those for the uniform half-space. For a three-layered structure, the total fields (including the DR waves, lateral wave, and trapped surface wave) are plotted in Figure 10 with the relative permittivity and electric length of the intermediate dielectric chosen as $\varepsilon_{r1} = 2.65$, and $k_1 l_1 = 0.45\pi$, respectively. It is seen that the DR wave, lateral wave, and the trapped surface wave are combined in the total field to produce an interference pattern.

In order to investigate the properties of the electromagnetic field, the total field (including the DR waves, lateral wave, and trapped surface wave) is computed in Figures 11(a) and 11(b), respectively. The lateral wave and trapped surface wave are computed in Figures 11(c) and 11(d), respectively. The computation coefficients of relative permittivity in the intermediate dielectrics are chosen as the same in Figures 5(c) and 5(d), while each electric length of the intermediate dielectrics are

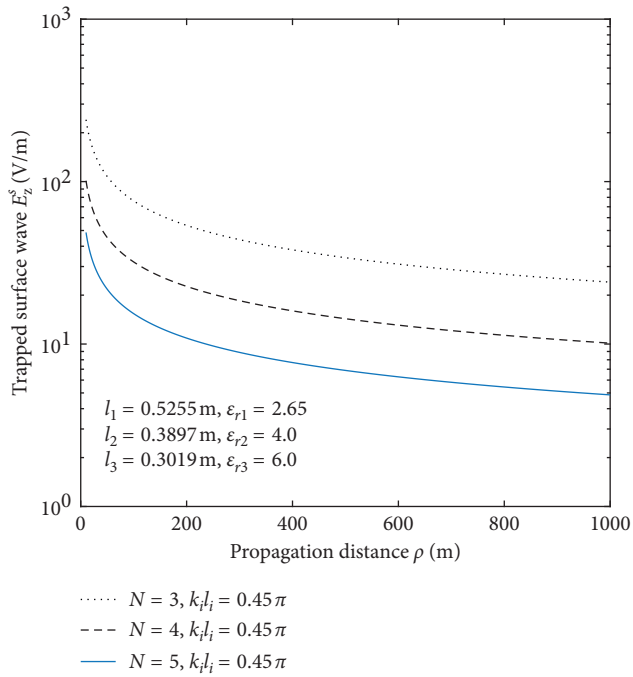

Figure 8: The electric component of trapped surface wave $|E_{0z}^S(\rho, z)|$ generated by a vertical dipole in the presence of three-layered to five-layered regions.

Table 1: Comparison of computational feasibility and complexity for root finding algorithms. (n: represents the order of computations).

Method	Analytical solution by graphical approach	Computation complexity of root finding algorithm	Nested recursion
Three-layered case	In lossless case	Easy	1
Four-layered case	In lossless case	Complicated	2
$N \geq 5$	Unavailable	Complicated	$N-2$
$N \leq 6$ by proposed equations (25)–(28)	In lossless case	Easy	0
$N > 6$ by proposed equations (23) and (24)	In lossless case	Complicated	0

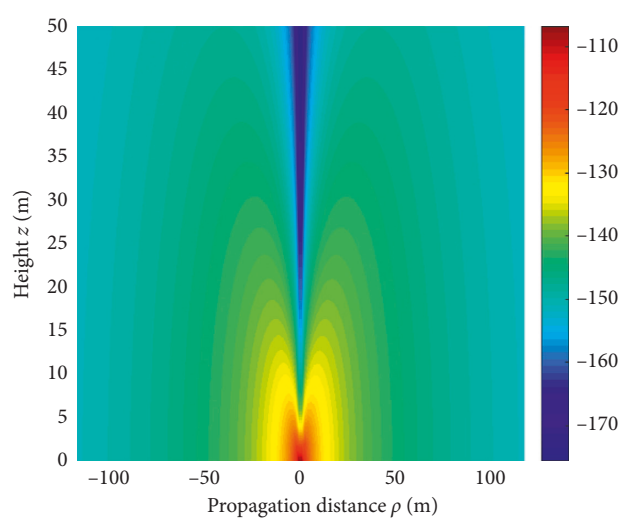

Figure 9: Spatial distributions in $\widehat{\rho} - \widehat{z}$ plane of the DR terms of the magnetic field component $|B_{0\phi}|$ in dB due to a vertical electric dipole in the presence of N-layered regions.

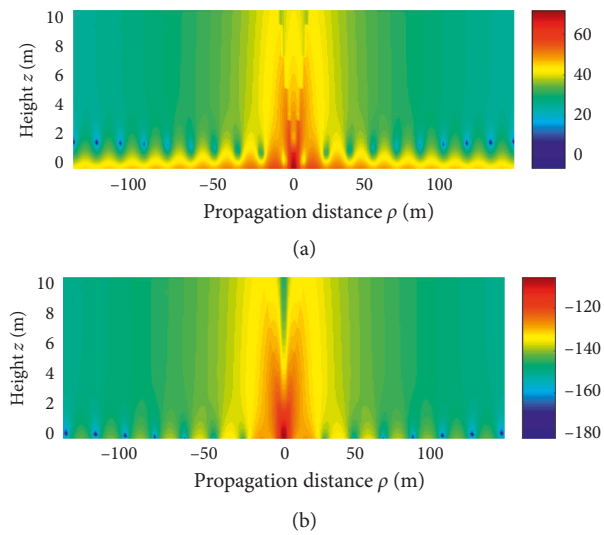

Figure 10: Spatial distributions in $\hat{\rho} - \hat{z}$ plane of the electromagnetic field in dB due to a vertical electric dipole above a dielectric-coated conductor. (a) $|E_{0z}(\rho, z)|$ and (b) $|B_{0\Phi}(\rho, z)|$.

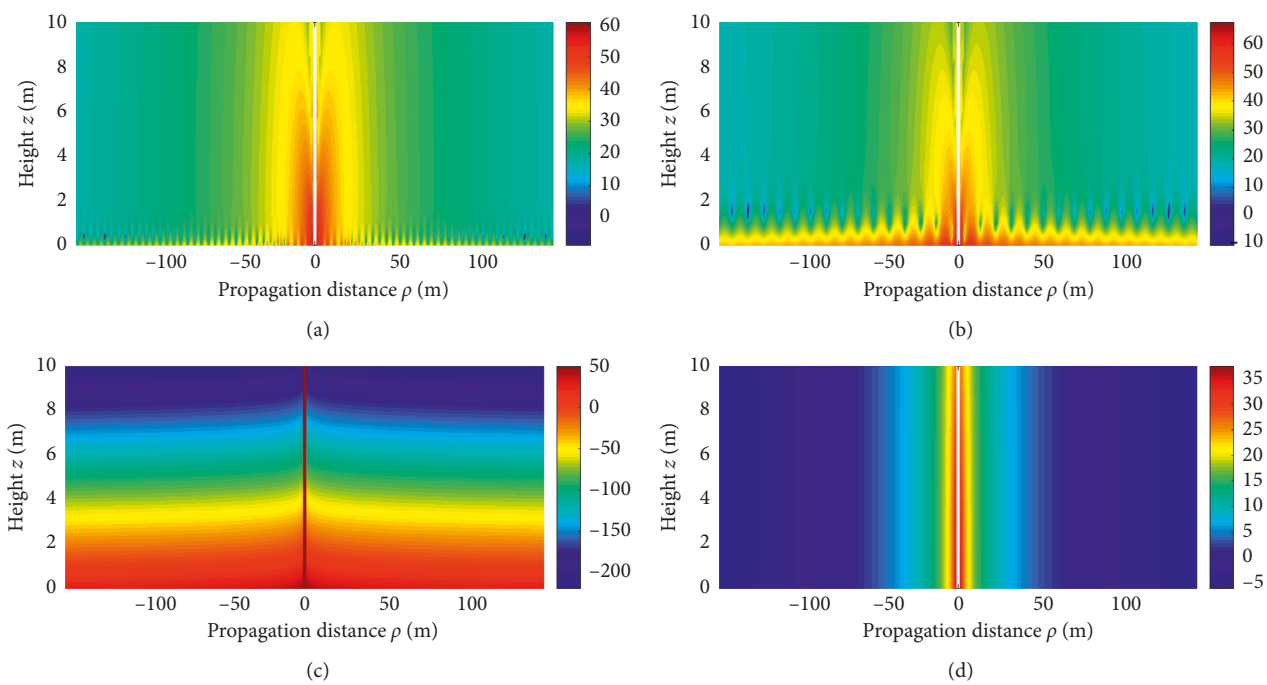

Figure 11: Spatial distributions in $\hat{\rho} - \hat{z}$ plane of the electric field $|E_z(\rho, z)|$ in dB due to a vertical electric dipole above the conductor coated by two dielectric layers at $f = 100$ MHz; $\varepsilon_{r1} = 2.65$, $\varepsilon_{r2} = 4$, and $z = d = 0$ m with (a) $k_1 l_1 = k_2 l_2 = 0.45\pi$; (b) $k_1 l_1 = k_2 l_2 = 1.45\pi$; (c) trapped surface wave; and (d) lateral wave.

chosen by $k_i l_i = 0.45\pi$ and $k_i l_i = 1.45\pi$, respectively. It is seen from Figures 11(c) and 11(d) that in the $\hat{z}$ direction and the trapped surface, wave attenuates rapidly away from the surface of air and dielectrics.

5. Conclusion

In summary, a computational scheme is presented to evaluate the residue sums for the fields of a vertical electric dipole oriented perpendicular to a stratified medium. The pole equation is reconstructed with explicit expression in the presence of the N-layered region. Therefore, a set of explicit equations is derived to enable analytical solutions on roots finding algorithms. Computations and analysis of electromagnetic field and its spatial distributions are carried out on and above a planar multidielectric-coated perfect conductor. The lateral wave and the trapped surface wave are combined in the total field to produce an interference pattern. It has been shown how the proposed equations are accurate and have significantly less computation complexity than previous numerical procedures.

Appendix

The coefficients in $A_1(\lambda)$ to $A_3(\lambda)$ and $B_1(\lambda)$ to $B_3(\lambda)$ are defined as follows:

$$
\begin{aligned}
A_1(\lambda) &= \frac{\gamma_0 k_1^2}{\gamma_1 k_0^2},\\
B_1(\lambda) &= \frac{\gamma_1 k_0^2}{\gamma_0 k_1^2},\\
A_2(\lambda) &= \frac{\gamma_0 k_2^2}{\gamma_2 k_0^2} - \frac{\gamma_1 k_2^2}{\gamma_2 k_1^2}\cdot \tan(i\gamma_1 l)\\
&\quad + \frac{\gamma_0 k_1^2}{\gamma_1 k_0^2}\cdot \tan(i\gamma_1 l)\cdot \tan(i\gamma_2 l),\\
B_2(\lambda) &= \frac{\gamma_2 k_0^2}{\gamma_0 k_2^2} - \frac{\gamma_2 k_1^2}{\gamma_1 k_2^2}\cdot \tan(i\gamma_1 l)\\
&\quad + \frac{\gamma_1 k_0^2}{\gamma_0 k_1^2}\cdot \tan(i\gamma_1 l)\cdot \tan(i\gamma_2 l),\\
A_3(\lambda) &= \frac{\gamma_0 k_3^2}{\gamma_3 k_0^2} - \frac{\gamma_1 k_3^2}{\gamma_3 k_1^2}\cdot \tan(i\gamma_1 l)\\
&\quad - \frac{\gamma_2 k_3^2}{\gamma_3 k_2^2}\cdot \tan(i\gamma_2 l) + \frac{\gamma_0 k_2^2}{\gamma_2 k_0^2}\cdot \tan(i\gamma_2 l)\cdot \tan(i\gamma_3 l)\\
&\quad + \frac{\gamma_2 k_3^2}{\gamma_3 k_2^2}\cdot \frac{\gamma_0 k_1^2}{\gamma_1 k_0^2}\cdot \tan(i\gamma_2 l)\cdot \tan(i\gamma_1 l)\\
&\quad + \frac{\gamma_0 k_1^2}{\gamma_1 k_0^2}\cdot \tan(i\gamma_1 l)\cdot \tan(i\gamma_3 l)\\
&\quad - \frac{\gamma_1 k_2^2}{\gamma_2 k_1^2}\cdot \tan(i\gamma_1 l)\cdot \tan(i\gamma_2 l)\cdot \tan(i\gamma_3 l),\\
B_3(\lambda) &= \frac{\gamma_3 k_0^2}{\gamma_0 k_3^2} - \frac{\gamma_3 k_1^2}{\gamma_1 k_3^2}\cdot \tan(i\gamma_1 l)\\
&\quad - \frac{\gamma_3 k_2^2}{\gamma_2 k_3^2}\cdot \tan(i\gamma_2 l) + \frac{\gamma_2 k_0^2}{\gamma_0 k_2^2}\cdot \tan(i\gamma_2 l)\cdot \tan(i\gamma_3 l)\\
&\quad + \frac{\gamma_3 k_0^2}{\gamma_0 k_3^2}\cdot \frac{\gamma_1 k_2^2}{\gamma_2 k_1^2}\cdot \tan(i\gamma_1 l)\cdot \tan(i\gamma_2 l)\\
&\quad + \frac{\gamma_1 k_0^2}{\gamma_0 k_1^2}\cdot \tan(i\gamma_1 l)\cdot \tan(i\gamma_3 l)\\
&\quad - \frac{\gamma_2 k_1^2}{\gamma_1 k_2^2}\cdot \tan(i\gamma_1 l)\cdot \tan(i\gamma_2 l)\cdot \tan(i\gamma_3 l).
\end{aligned}
\tag{A.1}
$$

Data Availability

The data used to support the findings of this study are available from the corresponding author upon request.

Conflicts of Interest

The authors declare that they have no conflicts of interest.

Acknowledgments

This work was supported by the National Natural Science Foundation of China under Grant number 61490695.

References

[1] V. Koju and W. M. Robertson, "Leaky Bloch-like surface waves in the radiation-continuum for sensitivity enhanced biosensors via azimuthal interrogation," *Scientific Reports*, vol. 7, no. 1, p. 3233, 2017.

[2] A. Delfan, M. Liscidini, and J. E. Sipe, "Surface enhanced Raman scattering in the presence of multilayer dielectric structures," *Journal of the Optical Society of America B*, vol. 29, no. 8, pp. 1863–1874, 2012.

[3] W. Y. Pan and K. Li, "ELF wave propagation along sea-rock boundary and mCSEM method," in *Propagation of SLF/ELF Electromagnetic Waves*, pp. 201–207, Zhejiang University Press, Springer-Verlag, Heidelberg, Germany, 1st edition, 2014.

[4] K. Li, S. O. Park, and H. Q. Zhang, "Electromagnetic field over the spherical Earth coated with *N*-layered dielectric," *Radio Science*, vol. 39, no. 2, pp. 1–10, 2004.

[5] J. R. Wait, *Electromagnetic Waves in Stratified Media*, Pergamon Press, New York, NY, USA, 2nd edition, 1970.

[6] R. W. P. King, M. Owens, and T. T. Wu, *Lateral Electromagnetic Waves: Theory and Applications to Communications, Geophysical Exploration, and Remote Sensing*, Springer, New York, NY, USA, 1992.

[7] A. Sommerfeld, "Propagation of waves in wireless telegraphy," *Annalen der Physik*, vol. 333, no. 4, pp. 665–736, 1909.

[8] D. Margetis and T. T. Wu, "Exactly calculable field components of electric dipoles in planar boundary," *Journal of Mathematical Physics*, vol. 42, no. 2, pp. 713–745, 2001.

[9] J. R. Wait, "Comment on "The electromagnetic field of a vertical electric dipole in the presence of a three-layered region" by Ronold W. P. King and Sheldon S. Sandler," *Radio Science*, vol. 33, no. 2, pp. 251–253, 1998.

[10] S. F. Mahoud, R. W. P. King, and S. S. Sandler, "Remarks on "The electromagnetic field of a vertical electric dipole over the earth or sea" [and reply]," *IEEE Transactions on Antennas and Propagation*, vol. 47, no. 11, pp. 1745–1747, 1999.

[11] R. E. Collin, "Hertzian dipole radating over a lossy earth or sea: some early and late 20th-century controversies," *IEEE Antennas and Propagation Magazine*, vol. 46, no. 2, pp. 64–79, 2004.

[12] R. E. Collin, "Some observations about the near zone electric field of a Hertzian dipole above a lossy earth," *IEEE Transactions on Antennas and Propagation*, vol. 52, no. 11, pp. 3133–3137, 2004.

[13] H. Q. Zhang and W. Y. Pan, "Electromagnetic field of a vertical electric dipole on a perfect conductor coated with a dielectric layer," *Radio Science*, vol. 37, no. 4, pp. 1–7, 2001.

[14] Y. H. Xu, W. Ren, L. Liu, and K. Li, "Trapped surface wave and lateral wave in the presence of a four-layered region," *Progress in Electromagnetics Research*, vol. 82, pp. 271–285, 2008.

[15] Y. L. Lu, Y.-L. Wang, Y. H. Xu, and K. Li, "Electromagnetic field of a horizontal electric dipole buried in a four-layered region," *Progress in Electromagnetics Research B*, vol. 16, pp. 247–275, 2009.

[16] K. Li, *Electromagnetic Fields in Stratified Media*, Zhejiang University Press, Springer-Verlag, Heidelberg, Germany, 2009.

[17] J. R. Wait, "Excitation of surface waves on conducting, stratified, dielectric-clad, and corrugated surfaces," *Journal of Research of the National Bureau of Standards*, vol. 59, no. 6, pp. 365-366, 1957.

[18] J. D. Cross and P. R. Atkins, "Electromagnetic propagation in four-layered media due to a vertical electric dipole: a clarification," *IEEE Transactions on Antennas and Propagation*, vol. 63, no. 2, pp. 866–870, 2015.

[19] Z. He and R. S. Chen, "A fast marching-on-in-degree solution for analysis of conductors coated with thin dispersive dielectric," *IEEE Transactions on Antennas and Propagation*, vol. 65, no. 9, pp. 4751–4758, 2017.

[20] S. He, Z.-P. Nie, and J. Hu, "Numerical solution of scattering from thin dielectric-coated conductors based on TDS approximation and EM boundary conditions," *Progress in Electromagnetics Research*, vol. 93, pp. 339–354, 2009.

[21] Z. He, D. Z. Ding, and R. S. Chen, "An efficient marching-on-in-degree solver of surface integral equation for multilayer thin medium-coated conductors," *IEEE Antennas and Wireless Propagation Letters*, vol. 15, pp. 1458–1461, 2016.